UCRL-91461
PREPRINT

PARAMETERIZATION OF A TRANSIENT ELECTROMAGNETIC FACILITY AND TEST ANTENNAS FROM TRANSIENT DATA

R. M. Bevensee
J. V. Candy
G. A. Clark
L. C. Martin
R. J. King

This paper was prepared for submittal to
Instrumentation Measurement Technology Conference
Tampa, FL
March 21-22, 1985

December 1984

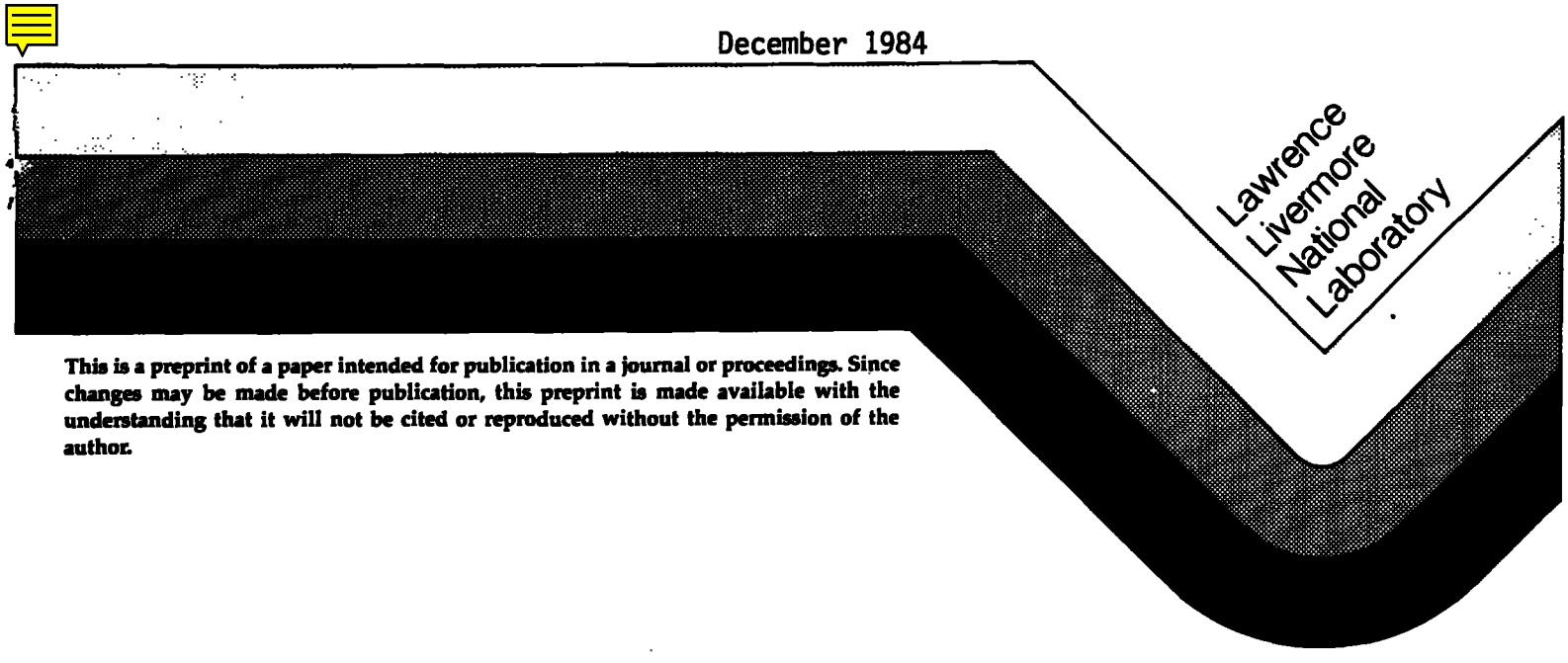

PARAMETERIZATION OF A TRANSIENT ELECTROMAGNETIC FACILITY AND TEST ANTENNAS FROM TRANSIENT DATA

R. M. Bevensee, J. V. Candy, G. A. Clark, L. C. Martin, and R. J. King

Lawrence Livermore National Laboratory, Livermore, California 94550

The Lawrence Livermore National Laboratory is characterizing antennas in their environments from transient reflectometry and scatter data taken on an Electromagnetic Transient Facility (EMTF). This paper describes the linear-system ARMAX modeling of the entire EMTF and derivation of the frequency-domain equivalent circuit of an antenna at its load port.

The EMTF is decomposed into blocks and model identification of each is achieved by data preprocessing, model-order testing, parameter estimation, prediction error tests for "fit" validation, and finally ensemble data tests on a well-understood electromagnetic dipole for overall EMTF model validation.

Various special ARMAX methods for modeling the equivalent circuit are compared, with emphasis on a special nonlinear least-squares algorithm. Data processing rules are given. Results for a 30 cm monopole antenna are presented.

Problems are summarized in the conclusions.

MODELING THE EMTF [1]

Figure 1 shows a schematic of the facility with the various components involved in the measurement of the load-port parameters of a test antenna. The associated equipment, consisting of monocone transmitting antenna of TEM impedance about 50 ohms, impulse pulser, sampling scope, delay line from the load port to the sampling scope, and data processing equipment, is shown below the ground plane.

Identification of a component in Fig. 1 is accomplished by (1) data preprocessing, (2) model order testing, (3) parameter estimation, (4) prediction error tests for "fit" validation, and (5) ensemble tests for model validation.

The pulse generator output is modeled by low-pass filtering and decimating the average of ten output waveforms. The generator "input" is modeled as an impulse of amplitude equal to the peak output. By ARMAX (N_A, N_B, N_C) modeling (autoregressive moving-average with exogenous input) the input u(t) and output y(t) are related as

$$A(q^{-1})y(t) = q^{-d}B(q^{-1})u(t) + C(q^{-1})e(t) \quad , \qquad (1)$$

where A, B, and C are polynomials in the backward shift operator q^{-1} of order N_A, N_B, and N_C, d is a delay, and e(t) is white noise [2,3,4]. This model yields the minimum error variance estimate of the unknown parameters and also the model order. From the estimated pulse $V_p(t)$ several statistics are computed to validate the parameters. Pulser terminal impedance Z_p is considered known.

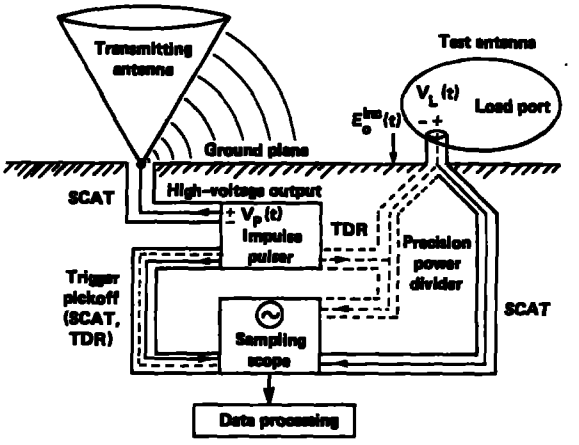

Fig. 1. Schematic of the EMTF, showing the signal paths for a TDR measurement (dashed lines) of test antenna input impedance Z_A at the load port and a scattering measurement (solid lines) of voltage V_L induced at the port. Different pulsers and delay lines between load port and sampling scope are used in the TDR and SCAT modes.

The reference field E_o^{inc} at the target was launched by a 180° wire screen configured to form a biconical horn radiating a spherical TEM mode above the ground plane. E_o^{inc}/V_p was quite accurate except in the low frequency range < 100 MHz and the high range > 2.5 GHz. (The newest transmitter is a full 360° sheet metal structure, with frequency response to 10 GHz, and a microwave absorber shroud to minimize high-frequency scattering. Clear time at the target is essentially infinite.)

E_o^{inc} is measured with no test antenna and the measurement cable terminated with a $\dot{D}$ probe to

record $\varepsilon\partial E/\partial t$. The probe transfer function was modeled with the bicone-characterized incident field as the probe input and a measured probe output as the output process.

The sampling scope is modeled as having a wideband frequency response. The delay line from load port to sampling scope (including the power divider in the TDR mode) is modeled only as a delay line.

The combined model of transmitting antenna and $\dot{B}$ probe was validated as follows. By deconvolving the probe response from the free-space (no test antenna) output one compares the free-space probe input with E_0^{inc} generated by the bicone transmitter model. One obtains this probe input $\hat{u}(t)$ from the ARMAX model inverse to (1):

$$\hat{u}(t) = [b_0 - B(q^{-1})]\hat{u}(t - i) + A(q^{-1})y(t) \quad , \quad i = 1, \ldots, N_B \qquad (2)$$

It was found that the procedure worked quite well, in that the noisy $\hat{u}(t) \approx u(t)$ of the identified transmitter response, until the latter fell below the noise level.

After the EMTF components were characterized the overall signal processing capability was validated by measurements on a well-understood electromagnetic dipole. From the final measurements at the sampling scope the dipole output $y(t)$ was obtained by deconvolution, and this along with its known input $u(t)$ yielded the complex pole frequencies s_i and natural mode amplitudes η_i in a Singularity Expansion Method (SEM) representation of the dipole output at point $\bar{r}$:

$$y(\bar{r},t) = \sum_i \nu_i(\bar{r})e^{s_i t}\eta_i(E^{inc}, s_i)u(t) \quad , \qquad (3)$$

where ν_i = natural mode response of the body and η_i = coupling coefficient measuring the strength of the oscillation. The agreement between the s_i so obtained and the theoretical values served as a measure of the overall validation.

However, one should beware of attaching too much physical significance to a pole-zero set of complex frequencies for a general test antenna. The poles identified by black-box methods are not unique.

The details of this overall validation now follow. A test dipole was used as the "known" test object for validation purposes. After the dipole response was acquired with the sampling scope, the EMTF models were used to extract both input and output signals for the ARMAX algorithms. Initially, the noise was ignored and an ARMAX (15, 12, 0) model, Eq. (1), was fit using least-squares techniques to provide initial parameter estimates for three algorithms: Recursive Extended Least Squares (RELS), Recursive Maximum Likelihood (RML), and off-line Nonlinear Iterative Least Squares (NLS). NLS uses linear pole-zero modeling, a mean-square output error criterion, and iterative nonlinear programming.

Each algorithm was run over the dipole data, producing pole estimates (damping and frequency). The estimated poles were compared to those theoretically predicted for that dipole [5]. All three algorithms yielded a reasonable "fit" to the data, i.e., the identified time responses and spectra matched those of the data. The estimates of the frequency portions of the odd $s_1, s_3, \ldots, s_{11}$ so obtained were quite good, although poorer for the higher s_i; the damping portions were not well estimated.

It was concluded that validation of the entire EMTF relative to this known test dipole was reasonable according to the basic dipole model extracted from the noisy data. One can then infer that knowledge of the noisy free-field input $E_0^{inc}(t)$ and ability to deconvolve the measured noisy output at the sampling scope to obtain the noisy output of a test object enables one to obtain accurate information for deriving the equivalent circuit of this object. The procedure for doing this is described next.

EQUIVALENT CIRCUIT OF A TEST ANTENNA [6]

Figure 2 shows the circuit in the complex frequency s-domain at its load port, from which the response of any linear load $Z_L(s)$ to any incident field $E^{inc}(s)$ (with the same spatial structure as the calibrating E_0^{inc}) can be computed once Z_A and h_{eff} are obtained. If the test antenna is a scale model version of the actual one characterized by Z_A, h_{eff}, these are found at real frequencies, neglecting surface loss, as: $Z_A(f) = Z_A(Kf)$, $h_{eff}(f) = K\, h_{eff}(Kf)$, $K > 1$ being the scale factor.

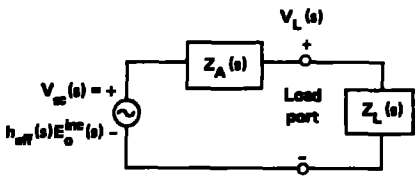

Fig. 2. Complex-frequency equivalent circuit of the test antenna at the load port. Z_A is determined by a TDR measurement; h_{eff}, by a scattering measurement. E_0^{inc} is at a reference point near the antenna. Z_L is the input impedance of the measurement cable.

$Z_A(s)$ is determined from a TDR measurement in Fig. 1 with a cable of impedance $Z_L = Z_0$ connected directly to the load port. This avoids the use of an awkward $\dot{B}$ current probe with a restrictive frequency response. The reflection coefficient $\rho(s) = V_L(s)/V_0(s)$ is obtained from measurement, whence

$$Z_A(s) = Z_0\frac{1 + \rho(s)}{1 - \rho(s)} = Z_0\frac{V_0(s) + V_L(s)}{V_0 - V_L} \quad . \qquad (4)$$

$V_0(t)$ is recorded with the test body absent (open-circuit); $V_L(t)$, with it present; then both $(V_0(t) \pm V_L(t))$ are transformed to the s-domain. Once $Z_A(s)$ is known, $h_{eff}(s)$ is obtained from a scatter (SCAT) measurement of $V_L(s)$ with the test antenna in position in Fig. 1:

$$h_{eff}(s) = \frac{V_L(s)}{E^{inc}(s)} \frac{Z_A(s) + Z_o}{Z_o} \quad , \qquad (5)$$

$E^{inc}(s)$ having been parameterized as described.

Both TDR and SCAT data are sampled with a TEK 7854 scope with a maximum resolution of 1024 points/waveform. It averages many waveforms to reduce noise. The performance criterion for Z_A- and h_{eff}-modeling is mean-square error.

Of the two types of errors, output and equation, it is generally believed that the former has more physical meaning. Output error, the difference between actual and estimated output, is quadratic for the all-zero, moving average FIR (finite impulse response) model, implying a unique minimum exists, but is nonquadratic for IIR modeling. IIR (infinite impulse response) modeling can be all-pole AR (autoregressive) or pole-zero ARMA (autoregressive moving-average) [2,7]. Equation error, the difference between actual output and a function of the model parameters, is synonymous with output error for a FIR model but different for an IIR model. A unique error minimum is guaranteed in either case.

FIR and recursive IIR modeling have been disappointing. The former applied to obtain a transfer function like ρ has these problems: (1) it does not distinguish between input signal and noise, (2) the model becomes large, (3) nonrealistic zero-padding is required for computation of correlations. Recursive IIR modeling generally doesn't work well on transient data, of which large amounts are required. Iteration has been disappointing.

The advantages of using NLS for either FIR or IIR modeling are (1) use of output error as the criterion of accuracy, (2) it is iterative rather than recursive, (3) it is manageable on a VAX computer, and (4) it produces a parametric model with natural poles and zeros. The disadvantages are that it does not model noise separately and encounters problems with zeros in the input data spectrum.

These various identification algorithms perform better when the data are not sampled beyond the Nyquist rate. An output time record should be aligned with the input record. If a time record is truncated too short, the discrete Fourier transform can contain "leakage" from higher frequencies into the measurable range. This is reducible by using a tapered window, and there are basic rules for either a tapered or rectangular one.

The procedure for characterizing Z_A of a test antenna runs as follows with a 30 cm monopole as an example. The TDR data are preprocessed by aligning the time records of $V_o(t)$ and $V_L(t)$, then windowing and low-pass-filtering $(V_o - V_L)$ and $(V_o + V_L)$, after which the Fourier transforms are taken. Ordinary f-domain division is performed in Eq. (4). FIR modeling of order 128 is performed with NLS and the high frequency artifacts are removed by low-pass Butterworth filtering. IIR modeling with NLS is also performed, once with a 20^{th} order model and once with a 6^{th} order one. The former fit the data (including the noise) more closely but contained high-frequency artifacts. The 6^{th} order model is probably adequate for most purposes, though its magnitude was low at low frequencies.

h_{eff} is characterized by first integrating $E^{inc}_{meas}(t)$ (measured with a $\dot{D}$ probe) to obtain $E^{inc}_{o}(t)$. This was low-pass filtered with an 8^{th} order Butterworth filter, decimated (Δt increased to $1/2\ f_{max}$), then Fourier transformed to yield $E^{inc}_{o}(f)$. $V_L(f)$ in Figs. 1 and 2 was obtained similarly. Then ordinary f-domain division was performed in (5), as well as FIR modeling like that for Z_A and IIR modeling with NLS of orders 20, 10, and 6. Again, the higher-order models fit the noisy data better but contained more high-frequency artifacts.

For both the Z_A- and h_{eff}- modeling the curves of magnitude vs. f obtained by f-domain division, FIR modeling and 6^{th} order IIR modeling agreed well with each other except at low frequencies, where the IIR curve was appreciably lower than others. See Figs. 3 and 4.

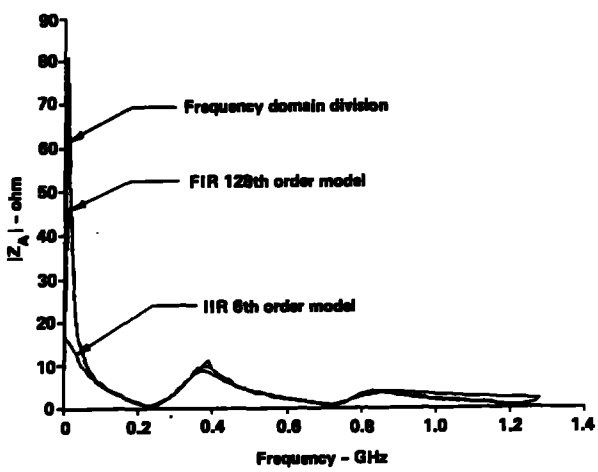

Fig. 3. Overlay of the normalized impedance transfer functions estimated using three different methods.

CONCLUSIONS

Data preprocessing of the sort described above is essential. The EMTF presently needs anti-aliasing filters to avoid the foldback of high-frequency noise into the measurable band determined by the sampling rate. Computational difficulties arise when a model order is too large, indicating that SEM poles should be discarded if they do not contribute significantly to the response of a component or test antenna. ARMAX modeling with NLS so as to include noise according to Eq. (1) might be the best technique of all.

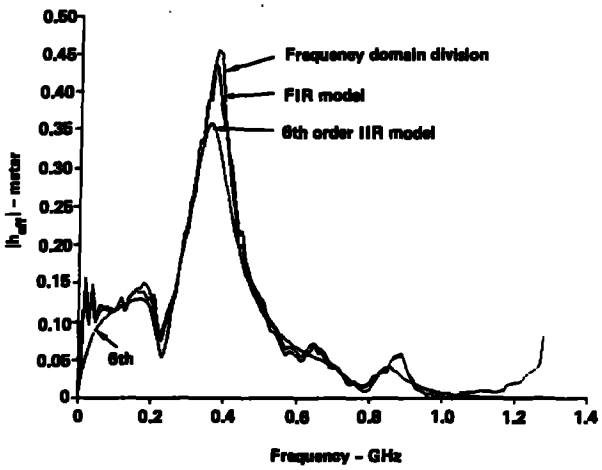

Fig. 4. Overlay of the effective height transfer functions calculated using three different methods.

REFERENCES

[1] J. E. Zicker and J. V. Candy, "Electromagnetic Test Facility Characterization: An Identification Approach," UCID-19620, Lawrence Livermore National Laboratory, December, 1982.

[2] L. Ljung and T. Soderstrom, Theory and Practice of Recursive Identification, Cambridge, MA: MIT Press, 1983.

[3] Automatica, Special Issue on Identification and Parameter Estimation, Pergamon Press, Jan., 1981.

[4] J. V. Candy and J. E. Zicker, "Identification of Electromagnetic Object Response From Noisy Transient Measurements," in IFAC Identification and System Parameter Estimation 1982, pp. 609-614, 1982.

[5] F. M. Tesche, "On the Analysis of Scattering and Antenna Problems Using the Singularity Expansion Technique," IEEE Trans. Ant. Prop., vol. AP-21, pp. 53-62, Jan., 1973.

[6] G. A. Clark, L. C. Martin, and E. J. Bogdan, "Identification of Antenna Parameters from Time-Domain Pulse Response Data," UCID-19770, Lawrence Livermore National Laboratory, April, 1983.

[7] D. M. Goodman, "NLS: A System Identification Package for Transient Signals," UCID-19767, Lawrence Livermore National Laboratory, March, 1983.

"Work performed under the auspices of the U.S. Department of Energy by the Lawrence Livermore National Laboratory under contract number W-7405-ENG-48."